RF DESIGN AND BEAM DYNAMICS OF A 3 GHZ SCDTL OPTIMIZED IN TERMS OF $(S_c^{\max}/E_a^2)/ZTT$ FOR CARBON ION ACCELERATION IN A MEDICAL INJECTOR

Eduardo Martinez-Lopez*, Nuria Fuster-Martínez, Março Boronat, Juan Carlos Fernández-Ortega, Daniel González-Iglesias, Juan Fuster, Benito Gimeno, Daniel Esperante
Instituto de Física Corpuscular, Paterna, Spain
Alexej Grudiev
European Organization for Nuclear Research (CERN), Geneva, Switzerland
Concepción Oliver
Department of Technology, CIEMAT, Avenida Complutense 40, Madrid, 28040, Spain

Abstract

This study presents a comprehensive methodology for the RF design and optimization of a 3 GHz SCDTL structure in terms of the modified Poynting vector S_c and the effective shunt impedance ZTT. By systematically refining the geometry of both accelerating and side-coupling cavities, the design achieves a maximized effective shunt impedance and accelerating gradient while ensuring compliance with breakdown limits based on the modified Poynting vector. The optimized structures are subsequently used to investigate beam dynamics constraints for a representative C^{6+} carbon ion beam, which is pre-accelerated in 750 MHz structures up to 10 MeV/u and then further accelerated in the proposed SCDTL structures from 10 MeV/u to 85 MeV/u.

INTRODUCTION

Hadron therapy is a cancer treatment modality that employs hadrons to irradiate tumors with high precision. To enable such fast and precise energy modulation, LINAC-based systems rely on a sequence of radio-frequency (RF) accelerating cavities, which transfer energy to the particles through oscillating electromagnetic fields. The design of low-energy accelerating structures should be primarily guided by the effective shunt impedance per unit length (ZTT), as it directly determines the energy efficiency of the system:

$$ZTT = \frac{\Delta W^2}{P_d \times L} \tag{1}$$

where ΔW is the energy gain, P_d is the dissipated peak power, and L is the active length of the LINAC.

For compact hadron therapy LINACs, the radio-frequency operating frequency $f_{\mathrm{RF}} = 3$ GHz has been established as the standard for accelerating structures operating above 10 MeV/u. At lower energies, however, a reduced RF frequency is required, with 750 MHz commonly adopted in several LINAC designs [1]. This choice is motivated by beam dynamics considerations: the RF defocusing scales as $\Delta p_{\mathrm{r}} \propto f_{\mathrm{RF}}/\beta^2\gamma^2$, while the longitudinal energy acceptance scales as $\omega_{\max} \propto \sqrt{\beta^3\gamma^3/f_{\mathrm{RF}}}$, where β is the particle velocity normalized to the speed of light and γ is the Lorentz factor [2].

The frequency transition is typically performed around 10 MeV/u [3–5]. The most efficient and widely used structure for this purpose is the 3 GHz SCDTL, which is commonly employed to accelerate ions from 10 to 100 MeV/u [1, 6, 7]. The SCDTL is composed of a series of short accelerating cavities interconnected by side-coupling cavities (SCCs) via coupling slots. The use of short cavities removes the requirement for post-coupler stabilization, thereby simplifying the overall structure [8].

This paper presents the design and optimization of 3 GHz SCDTL structures in terms of the figure of merit $(S_c^{\max}/E_a^2)/ZTT$, where S_c denotes the modified Poynting vector and E_a the effective accelerating gradient. The achievable accelerating gradients are evaluated, and the optimized structures are subsequently employed in beam dynamics studies. Special attention is given to longitudinal capture, particularly to the effects associated with the frequency transition from 750 MHz to 3 GHz.

THE RF CAVITIES

The accelerating and side-coupling cavities were designed separately to resonate at $f_{\mathrm{RF}} = 3$ GHz. The RF design optimization of the cavities was carried out using `SUPERFISH` [9, 10], applying the Slater perturbation method, and subsequently validated using full 3D electromagnetic simulations in `CST Microwave Studio` [11].

The RF Accelerating Cavity

Figure 1 shows the geometry of the accelerating cavity of a SCDTL structure designed to operate in the TM_{01} mode with a zero-mode field configuration and a cell length equal to $\beta\lambda$, where λ is the RF wavelength. The resonant frequency f_{RF} is primarily determined by the cavity diameter D. The inner radius of the drift tubes corresponds to the cavity aperture radius r. The initial and final cells, which contain the noses, have a length of $\beta\lambda/4$ each.

The RF Side-Coupling Cavity

The accelerating cavities are interconnected via side-coupling cavities (SCCs) through coupling slots. The length

* Corresponding author: Eduardo.Martinez@ific.uv.es

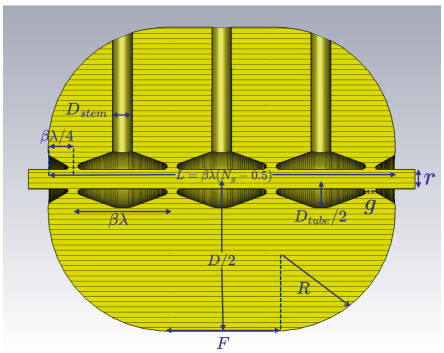

Figure 1: Geometry of a 3 GHz 4-gap accelerating cavity of a SCDTL structure

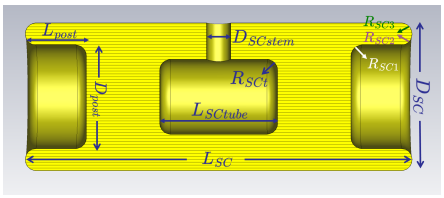

Figure 2: Geometry of a side-coupling cavity of a 3 GHz SCDTL structure

of the SCCs, L_{SC}, depends on the separation distance between the accelerating cavities, which in turn is determined by the space required to place quadrupole magnets for transverse beam focusing.

Figure 2 shows the design of the SCCs. The SCC, with diameter D_{SC}, is a figure of revolution that includes a central tuning post with length L_{post} and diameter D_{post}.

RF EFFICIENCY DESIGN

The robust and systematic optimization of the most relevant geometric parameters for both accelerating and coupling cavities is presented in [7]. Using the optimal parameter set with a bore radius of 2 mm, a ZTT value of up to 140 MΩ/m is achieved, with a coupling factor in the range of 3–4%.

FIELD LIMITS AND ACHIEVABLE GRADIENTS: MODIFIED POYNTING VECTOR CRITERION

Although the maximum surface electric field criterion has historically been used as a reference indicator for vacuum RF breakdown, it is now well established that the surface electric field alone does not provide a universal or reliable limit for high-gradient accelerating structures.

A more comprehensive description of RF breakdown limits was introduced by Grudiev, Calatroni, and Wuensch [12], who proposed a new local field quantity based on the electromagnetic power flow on the cavity surface. This quantity, known as the modified Poynting vector S_c, accounts for both the electric and magnetic field contributions involved in the breakdown triggering process and has been shown to provide a more consistent scaling of breakdown data across different frequencies, pulse lengths, and structure types.

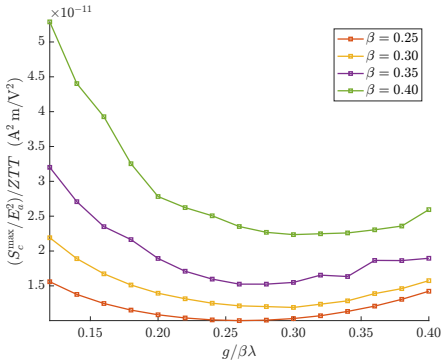

Figure 3: Ratio $(S_c^{max}/E_a^2)/ZTT$ as a function of the normalized gap length $g/\beta\lambda$ for different cell lengths in an optimized four-gap 3 GHz SCDTL structure

Table 1: Main Accelerating Parameters of the 3 GHz SCDTL Structure Optimized in Terms of $(S_c^{max}/E_a^2)/ZTT$ for Different Particle Velocities

Particle velocity, β	0.25	0.30	0.40
Normalized gap size, $g/\beta\lambda$	0.26	0.30	0.30
Design active accelerating gradient (MV/m) (S_c^{lim} = 0.4 MW/mm² criterion)	16.3	15.7	12.5
Max ratio E_{max}/E_a	9.2	9.5	11.6
Effective shunt impedance, ZTT (MΩ/m)	148.5	140.7	117.3

In practical RF optimization, this consideration naturally leads to the introduction of a combined figure of merit, $(S_c^{max}/E_a^2)/ZTT$, which balances breakdown robustness against RF efficiency. Figure 3 shows the ratio $(S_c^{max}/E_a^2)/ZTT$ as a function of the normalized gap length $g/\beta\lambda$ for different cell lengths in an optimized four-gap 3 GHz SCDTL structure.

Experimental results from a 3 GHz backward travelling wave (BTW) structure indicate a limiting value of S_c = 2.1 MW/mm² at a pulse length of 1.6 μs [13]. For long RF pulses typical of medical LINACs, these values have been rescaled to pulse lengths of several microseconds [13]. This rescaling leads to a limiting value of S_c^{lim} = 1.2 MW/mm² for copper cavities operating with pulse lengths around 5 μs and breakdown rates compatible with reliable clinical operation. In this work, a conservative limit of S_c^{lim} = 0.4 MW/mm² has been adopted, similar to the values used in optimized designs based on S_c [3, 14].

Table 1 summarizes the main accelerating parameters of the 3 GHz SCDTL structure for different particle velocities. The structure was optimized to minimize the figure of merit $(S_c^{max}/E_a^2)/ZTT$.

BEAM DYNAMICS RESULTS

A SCDTL employs a focusing lattice that approximates a FODO cell structure. However, this description is not strictly accurate, as the FODO cell length increases with the particle velocity β. Additionally, RF defocusing effects are present, and the particle momentum changes along the structure due to acceleration.

In SCDTL transverse beam dynamics, the designer should adopt the following methodology: first, a transverse match-

Table 2: Beam Dynamics Results for a Representative C^{6+} Beam Transported Through the Optimized 3 GHz SCDTL Structures for Different Bore Radius Values Over the Range $\beta = 0.15$–0.40

Optimized SCDTL Structure	Bore Radius r (mm)	Transverse Acceptance (π mm·mrad)	Energy Spread Acceptance (keV/u)	Emittance Growth $\sum \Delta\epsilon_i/\epsilon_i$
$\frac{S_c^{max}/E_a^2}{ZTT}$	2.0	9.5	271.7	0.16
	2.5	14.8	261.7	0.13
	3.0	21.7	250.9	0.11

ing section should be designed to achieve a phase advance of 90 degrees at the SCDTL entrance, with the aim of minimizing emittance growth. If the particle transmission is not adequate, it can be improved in two ways: by reducing the FODO cell length through the implementation of higher-gradient short magnets or by increasing the aperture radius.

For longitudinal constraints, the designer should consider implementing a buncher cavity to ensure proper longitudinal matching. An alternative lower-cost solution that avoids the use of a buncher cavity and additional components is to reduce the synchronous phase of the first SCDTL cavities until optimal longitudinal matching is achieved.

Beam dynamics simulations were performed using the `RF-Track` code [15]. A representative C^{6+} ion beam at 10 MeV/u was considered, previously accelerated from the source to 5 MeV/u by a 750 MHz RFQ and further accelerated to 10 MeV/u using 750 MHz IH cavities [4]. The normalized input transverse emittances at the exit of the 750 MHz IH structures are $\epsilon_{n,x} = 0.028$ π mm·mrad and $\epsilon_{n,y} = 0.027$ π mm·mrad, while the longitudinal emittance is $\epsilon_z = 0.141$ π deg·MeV. The remaining beam parameters are taken from the referenced work.

The transport of the representative C^{6+} beam in the $\beta = 0.15$–0.40 range is shown in Fig. 4, using the $(S_c^{max}/E_a^2)/ZTT$-optimized SCDTL structure with $r = 2$ mm, as described in Section . The beam dynamics is determined using a set of 5 cm long quadrupole magnets with gradients of up to 250 T/m. The Twiss parameters at the entrance of the SCDTL structure are derived from a 0.71 m long matching section composed of four quadrupoles, designed to achieve a phase advance close to 90 degrees within the SCDTL structure in order to minimize emittance growth. The synchronous phase increases linearly along the entire SCDTL linac from −25 to −20 degrees, except for the first cavity, where a synchronous phase of +10 degrees is used to achieve optimal longitudinal matching. Figure 5 shows the C^{6+} beam at the entrance of the SCDTL structure after the matching section. More than 98% of the beam is contained within the longitudinal acceptance of the $(S_c^{max}/E_a^2)/ZTT$-optimized SCDTL.

Table 2 summarizes the beam dynamics simulation results for the representative C^{6+} beam transported through the optimized 3 GHz SCDTL structures developed in this work. For each optimized structure, beam dynamics studies were performed considering different bore radius values in order to evaluate their impact on the beam dynamics. The accelerating gradients of the structures were recalculated as a function of the bore radius. All simulations were carried out following the same methodology used in the example shown in Fig. 4.

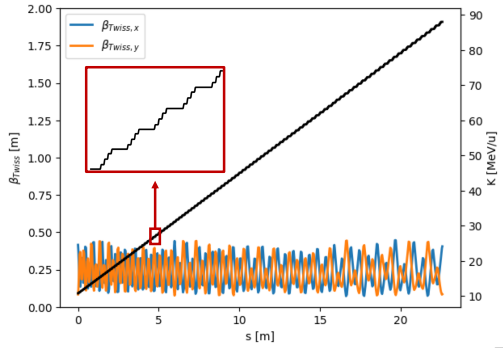

Figure 4: Representative C^{6+} beam transport through the $(S_c^{max}/E_a^2)/ZTT$-optimized SCDTL structure from 10 MeV/u to 88 MeV/u. Throughout the linac, the aperture radius ($r = 2$ mm) remains larger than $6\sigma_{x,y}$, where $\sigma_{x,y}$ denotes the transverse beam size

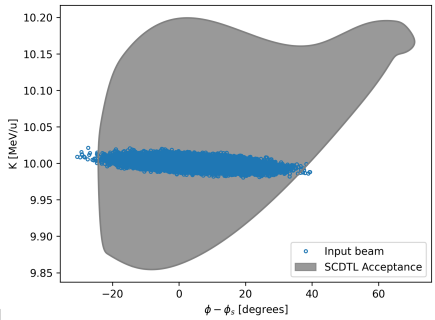

Figure 5: Longitudinal phase space distribution of the representative 10 MeV/u C^{6+} beam at the entrance of the $(S_c^{max}/E_a^2)/ZTT$-optimized SCDTL structure

CONCLUSION

In this work, a 3 GHz SCDTL structure with an aperture radius of $r = 2$ mm has been designed and optimized in terms of $(S_c^{max}/E_a^2)/ZTT$, achieving an effective shunt impedance of up to 150 MΩ/m and an active accelerating gradient of up to 16.5 MV/m.

Beam dynamics studies show that the optimized structures can accelerate a representative C^{6+} beam from 10 to 85 MeV/u with full transverse transmission and more than 98% longitudinal capture across the frequency transition from 750 MHz to 3 GHz.

ACKNOWLEDGEMENTS

The authors gratefully acknowledge the financial support provided by the PhD grant CIACIF/2022/109 and the research grant CDEIGENT/2021/012.

REFERENCES

[1] S. Benedetti, "New Trends in Proton and Carbon Therapy LINACs", in *Proc. LINAC'18*, Beijing, China, Sep. 2018, pp. 666–671. doi:10.18429/JACoW-LINAC2018-TH1P03

[2] T. P. Wangler, *RF Linear Accelerators*, 2nd ed., Wiley-VCH, Weinheim, Germany, 2008.

[3] S. Benedetti *et al.*, "High Gradient LINAC for Proton Therapy", *Phys. Rev. Accel. Beams*, vol. 20, p. 040101, 2017. doi:10.1103/PhysRevAccelBeams.20.040101

[4] J. Giner Navarro *et al.*, "KONUS Dynamics for a 750 MHz IH-Based Injector", *Nucl. Sci. Tech.*, vol. 37, p. 52, 2026.

[5] C. Ronsivalle *et al.*, "The TOP-IMPLART Project", *Eur. Phys. J. Plus*, vol. 126, p. 68, 2011. doi:10.1140/epjp/i2011-11068-x

[6] E. Martinez-Lopez *et al.*, "Design and Optimization of a 3 GHz SCDTL for Carbon Ion Acceleration in a Medical Injector", in *Proc. IPAC'25*, Taipei, Taiwan, 2025, pp. 1053–1055. doi:10.18429/JACoW-IPAC2025-TUPB039

[7] E. Martinez-Lopez *et al.*, "RF Design of 3 GHz SCDTL Structures for Ion Beams in Medical Accelerators", *Nucl. Eng. Technol.*, vol. 58, no. 8, 2026. doi:10.1016/j.net.2026.104361

[8] L. Picardi *et al.*, "Design Development of the SCDTL Structure for the TOP LINAC", *Nucl. Instrum. Methods Phys. Res. A*, vol. 425, no. 1–2, pp. 8–22, 1999. doi:10.1016/S0168-9002(98)01309-6

[9] J. H. Billen and L. M. Young, "POISSON SUPERFISH", Los Alamos National Laboratory Report LA-UR-96-1837, 2006.

[10] LANL Accelerator Code Group, "POISSON SUPERFISH User's Guide", Los Alamos National Laboratory Report LA-UR-96-1837, 1996.

[11] Dassault Systèmes, *CST Studio Suite*, 2023.

[12] A. Grudiev *et al.*, "New Local Field Quantity Describing the High-Gradient Limit of Accelerating Structures", *Phys. Rev. Spec. Top. Accel. Beams*, vol. 12, p. 102001, 2009. doi:10.1103/PhysRevSTAB.12.102001

[13] A. Vnuchenko *et al.*, "High-Gradient Testing of an S-Band Normal-Conducting Low Phase Velocity Accelerating Structure", *Phys. Rev. Accel. Beams*, vol. 23, p. 084801, 2020. doi:10.1103/PhysRevAccelBeams.23.084801

[14] P. Martinez-Reviriego *et al.*, "High-Power Performance Studies of an S-Band High-Gradient Accelerating Cavity for Medical Applications", *Nucl. Eng. Technol.*, vol. 57, p. 103164, 2025. doi:10.1016/j.net.2024.08.033

[15] A. Latina, "RF-Track: Beam Tracking in Field Maps Including Space Charge Effects", in *Proc. LINAC'16*, East Lansing, MI, USA, Sep. 2016.